PERGAMON

Electrochimica Acta 46 (2001) 3063–3071

ELECTROCHIMICA Acta

www.elsevier.com/locate/electacta

Double layer capacitance of Pt(111) single crystal electrodes

T. Pajkossy *, D.M. Kolb

Department of Electrochemistry, University of Ulm, D-89069 Ulm, Germany

Received 27 December 2000; received in revised form 21 February 2001

Abstract

In order to determine the double layer capacitance of the Pt(111) electrode, impedance and capacitance measurements were carried out in neutral and acidic aqueous perchlorate solutions. Separation of the double layer and adsorption contributions of the interfacial capacitance were based on the adsorption impedance theory. The double layer capacitance versus potential plot exhibits a peak at about 0.12 V versus SCE in the 1.5–7 pH range; from here towards cathodic potentials the capacitance attains a value of about 20 $\mu F/cm^2$. The peak may be related to the potential of zero free charge of the Pt(111) electrode. © 2001 Elsevier Science Ltd. All rights reserved.

Keywords: Platinum; Impedance; Double layer; Capacitance; Diffusion; Potential of zero charge

1. Introduction

The electrochemistry of platinum single crystals—especially of Pt(111)—has been intensively studied for about two decades, starting with the pioneering work of Clavilier et al. [1]. These studies have revealed that there are broad potential regions where adsorption of ions dominates the voltammetric behavior. For example, the hydrogen and hydroxide adsorption regions are the most characteristic features of the voltammograms measured in perchloric acid solutions. Between these regions there exists a rather narrow double layer region, for which it is assumed that the current is solely due to double layer charging. In general, we have little information about the double layer of platinum; therefore we have set ourselves the task of learning how to distinguish between double layer and adsorption contributions to impedance spectra of Pt(111) in simple aqueous electrolytes, and in particular, to determine the double layer capacity of this electrode.

2. Methods

The experimental set-up (instruments and software for cyclic voltammetry (CV), impedance, and capacitance measurements), the cell, chemicals, and all the experimental procedures were the same as used in our previous study of Au single crystals [2]; with the sole difference that during the present studies we employed a single-crystal Pt(111) electrode. This crystal was purchased from Mateck, Jülich, Germany; it was a cylinder of 4 mm diameter and 4 mm height with a platinum wire attached to the rear for mounting purposes. Before measurements, the electrode was annealed in a hydrogen or propane gas flame and, after cooling in nitrogen for about 1 min, it was immersed in water and thereafter transferred to the electrochemical cell with a protecting water droplet. Finally, the electrode was contacted with the electrolyte under potential control to yield the hanging meniscus configuration. We used a saturated calomel electrode (SCE) as reference; the potentials are given either versus SCE or versus reversible hydrogen electrode in the given solution

* Corresponding author. Research Laboratory of Materials and Environmental Chemistry, Chemical Research Center, Hungarian Academy of Sciences, Budapest, Pusztaszeri út 59-67, H-1025 Hungary.

E-mail address: pajkossy@chemres.hu (T. Pajkossy).

PII: S0013-4686(01)00597-7

(RHE). In order to prevent the solution from chloride contaminations, the SCE was placed in a separate compartment; a platinum wire in the main cell compartment connected to the SCE through a 4 μF capacitor ensured a good high-frequency behavior [3].

Cleanliness of the system was regularly checked by measuring voltammograms. The present level of cleanliness allowed us to perform a measurement series of about 20 min duration, and sometimes up to 2 h. This made it possible to measure 10–40 impedance spectra as a function of potential without re-annealing the electrode. The duration of experiments could be increased to some extent, if the potential was cycled once between 0.1 and 0.9 V versus RHE between two subsequent impedance spectrum measurements.

As in Ref. [2] the parameters of the appropriate equivalent circuit were calculated by fitting the impedance function to the measured spectra by a non-linear least squares program. The accuracy of the measured impedance spectra was about 1° of the phase angle and 1% of the magnitude at 10 kHz and about one order of magnitude better below 1 kHz, i.e. the spectra were fairly accurate. After performing the curve fitting, little if any systematic deviations of the measured and calculated spectra could be observed indicating that the fitting function is adequate; in general, the χ^2 values (residual mean squares) of the fits were between 10^{-5} and 10^{-4}, that is, the average deviation between measured and fitted points was less than 1%.

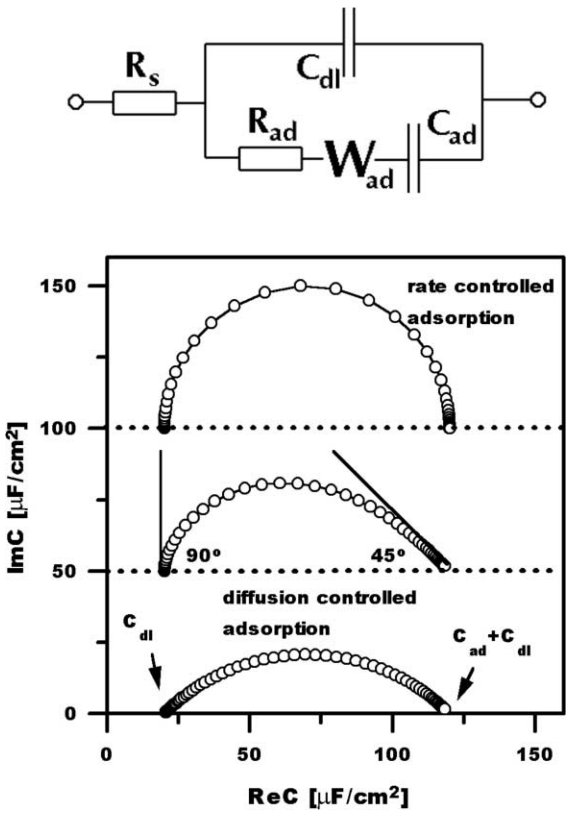

Fig. 1. (a) The equivalent circuit of the interface in the presence of adsorption. For notations see text following Eq. (1). (b) Capacitance spectra (with clockwise decreasing frequencies) due to adsorption at slow, medium and fast rates, calculated by using Eq. (1) and having the shapes of a semicircle, a skewed arc and a depressed arc, respectively. The spectra are shifted vertically for the sake of clarity.

The measured spectra are represented graphically throughout this work by calculating and plotting the $C(\omega) = Y(\omega)/(\mathrm{i}\omega) = 1/([Z(\omega) - Z(\omega \to \infty)]A_e\mathrm{i}\omega)$ complex function, where ω, $Z(\omega \to \infty) = R_s$, A_e, and i are the angular frequency, the solution resistance, the electrode area, and the imaginary unit, respectively. Because of its physical meaning $C(\omega)$ is termed the 'interfacial capacitance' and, being a complex quantity, can be plotted in complex representation (on a Nyquist-plot, being analogous to the Cole–Cole plot used in the context of dielectrics). Note that this representation highly exaggerates the deviations from the arc-shape at the high frequency end of the spectra. In the same vein, the capacitance–voltage curve consists of two parts: the Re C–E plot is the 'classical' C–E curve, whereas the Im C–E curve characterizes the 'loss' rather than the charge-storing behavior. These capacitance versus potential curves, $C(E)$, have been measured with a continuous potential scan at 10 mV/s; with applying a 1 kHz or 18 Hz, 10 mV peak-to-peak amplitude sinusoidal perturbation. The dc-capacitance, C_{dc}, is calculated by dividing the current density $j(E)$ by the sweep rate $v = \mathrm{d}E/\mathrm{d}t$. (We note that in preliminary experiments C_{dc} was found to be independent of sweep rate for the low sweep rates used.)

As preliminary experiments with many different solutions have revealed, one can measure the impedance spectra conforming to the circuit of Fig. 1a in the potential regions of specific adsorption, provided the adsorbate concentration is in the 0.1–1 mM range. The adsorption related elements of this circuit can be interpreted by the classical adsorption impedance theories elaborated by Ershler [4], Frumkin and Melik-Gaykasyan [5], and Lorenz [6], based on which we expect a capacitance spectrum, $C(\omega)$, of the form

$$C(\omega) = \frac{1}{\mathrm{i}\omega(Z(\omega) - R_s)} = C_{dl} + \frac{C_{ad}}{1 + \sigma_{ad}C_{ad}\sqrt{\mathrm{i}\omega} + R_{ad}C_{ad}\mathrm{i}\omega} \quad (1)$$

where C_{dl}, C_{ad}, and R_{ad}, stand for double layer and adsorption capacitances, and adsorption resistance, respectively, and σ_{ad} is the coefficient of the Warburg impedance, W_{ad}, defined by $Z(W_{ad}) = \sigma_{ad}(\mathrm{i}\omega)^{-1/2}$. The $C(\omega)$ spectra, plotted in the complex plane, are circular or distorted arcs (Fig. 1b); semicircles and 'depressed

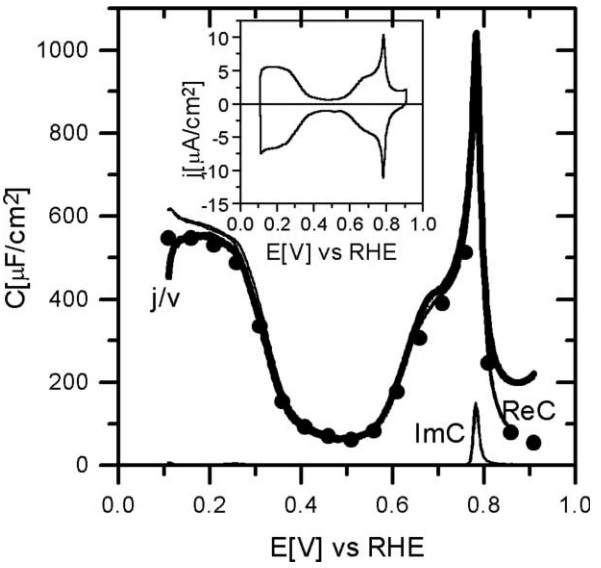

Fig. 2. Capacitance of Pt(111) in 0.1 M $HClO_4$ (pH 1) as function of potential. Circles: determined from impedance spectra in the 1 Hz–1 kHz frequency range. Errors bars are not drawn because they are smaller than the symbol size. Thin solid lines: real (Re C) and imaginary (Im C) components of the capacitance measured with 18 Hz and a potential scan of 10 mV/s. Thick solid line: DC capacitance, j/v. Inset: cyclic voltammogram at 10 mV/s, from which the DC capacitance has been calculated.

arcs' for the extremes of slow and fast adsorption, respectively. Independent of adsorption kinetics, the high and low frequency limits of the capacitance, C_{HF} and C_{LF} can be identified as C_{dl} and $C_{ad}+C_{dl}$; and these have the physical meaning of $C_{dl}=(\partial q^M/\partial E)_\Gamma$ and $C_{LF}=dq^M/dE$ where q^M and Γ stand for excess charge of the metal and surface excess of the adsorbate, respectively. The terms R_{ad}, and σ_{ad} represent the kinetics of the adsorption. Although we frequently found non-zero adsorption resistances, R_{ad}, in systems with certain adsorbing ions [7], in the systems of the present communication R_{ad} plays no role. For σ_{ad} one can show that [8]

$$\sigma_{ad}=\frac{RT}{\gamma^2F^2c_b\sqrt{D}} \tag{2}$$

where c_b, D, and γ are the bulk concentration, diffusion coefficient, and electrosorption valency [9] of the adsorbate, respectively, the other letters having their usual meaning. Combining Eqs. (1) and (2) and by ignoring the term containing R_{ad} we arrive at the following equation:

$$C(\omega)=C_{dl}+C_{ad}\left(1+\frac{RT}{\gamma^2F^2c_b\sqrt{D}}C_{ad}\sqrt{i\omega}\right)^{-1} \tag{3}$$

At constant C_{ad} (i.e. at constant coverage of the adsorbate), the second term increases with increasing adsorbate concentration. In other words (as it is demonstrated in Fig. 5 of Ref. [2]) the spectra shrink, towards the C_{HF} and C_{LF} points with decreasing and increasing bulk concentration of the adsorbate, respectively. A practical consequence of this behavior is that C_{HF} can be measured with good accuracy in solutions of low adsorbate concentrations within the easily accessible frequency range of 0.1 Hz to 5 kHz.

3. Results

The simplest and most frequently studied situation is Pt(111) in 0.1 M $HClO_4$ with the potential limited to the 0.1 to 0.9 V versus RHE range. The voltammogram of this system is shown in the inset of Fig. 2. Unfortunately, no information regarding the double-layer capacitance can be obtained with this system. To demonstrate this, we show in Fig. 2 capacitance–potential plots, which were determined by three different methods (a). We measured impedance spectra (in the 1 Hz to 10 kHz range) as a function of steady state potential. The measured spectra perfectly fit to the impedance function of a simple serial RC circuit; the calculated capacitance values are plotted as circles (b). The capacitance was measured during potential scans of 10 mV/s with constant 18 Hz perturbation (c). The dc capacitance was calculated from the anodic branch of the CV.

The capacitances determined by these three methods coincide fairly well; they are always much larger than 20 μF/cm² (which is usually considered to be typical for double layer capacitances) and can be regarded as typical adsorption capacitances. Note that at sufficiently high H^+ concentrations the equivalent circuit of Fig. 1 is simplified to $R_s(C_{dl}\|C_{ad})$ i.e. to a serial RC circuit (Eq. (3)). Hence we conclude that the double layer capacitance in strongly acidic solutions is completely masked by the adsorption-related capacitances; there is no way to separate them. However, for much lower H^+ concentrations, the separation is possible if we consider the following two properties of the voltammograms.

Firstly, the voltammetric features related to the hydrogen and hydroxide adsorption shift by -59 mV/pH [10]; apart from this horizontal shift, the shapes change only slightly. This means that the adsorption capacitances—and therefore also the coverages—measured in solutions of different pH values are approximately the same at a given potential against RHE. This feature allows us to vary the pH, while keeping coverages constant and to compare voltammograms and capacitances measured at different acidities.

Secondly, characteristic signs of diffusion control show up at sufficiently low concentrations of the adsorbate (H^+ and OH^-): the current becomes dependent on stirring and characteristic asymmetric CV features appear. Due to the role of diffusion, we obtain impedances well conforming to the adsorption impedance theory thereby allowing us to separate the two capacitances.

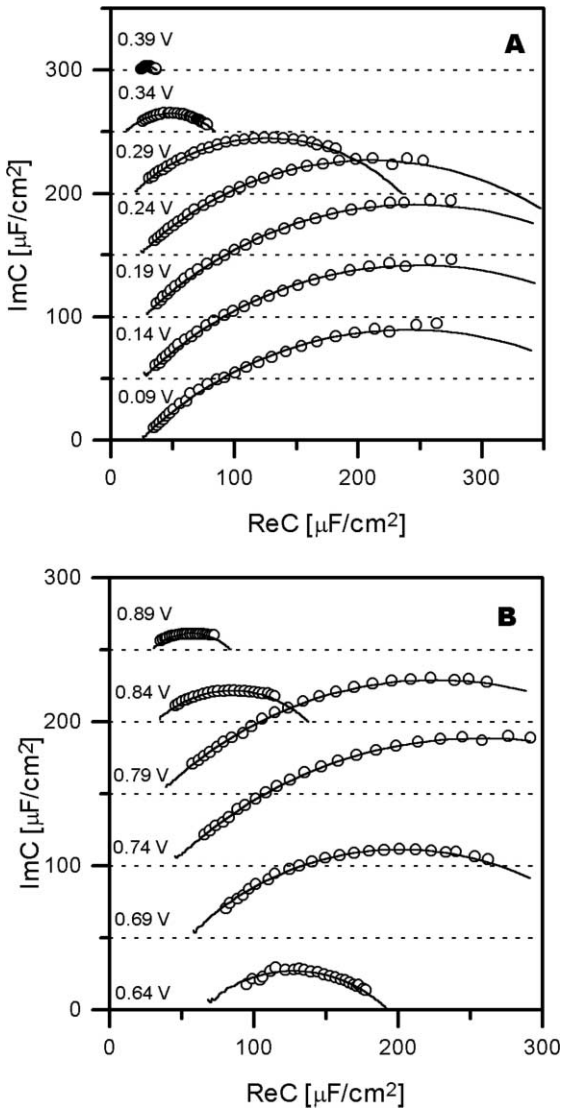

Fig. 3. Capacitance spectra (2 kHz–2 Hz clockwise) for Pt(111) electrode in 0.1 M $KClO_4 + 0.1$ mM $HClO_4$ solution (pH ≈ 4) at potentials (vs. RHE) as indicated (A, in the hydrogen adsorption region; B, in the hydroxide adsorption region). The spectra are shifted vertically for clarity. Note that the hf end of the spectra approach the ReC axis at 45° (rather than at right angles), indicating that in acidic solution the adsorption processes are immeasurably fast.

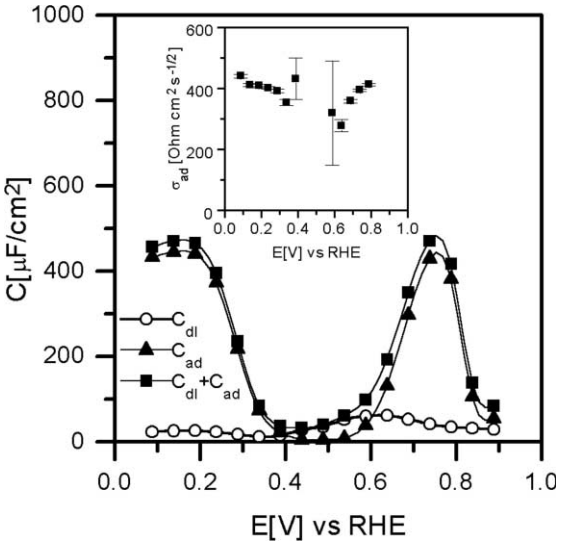

Fig. 4. Double layer capacitance, C_{dl}, adsorption capacitance, C_{ad}, and $C_{dl} + C_{ad}$ of Pt(111) in 0.1 M $KClO_4 + 0.1$ m M $HClO_4$ as function of potential. Errors bars of capacitances are not drawn because they are smaller than the symbol size. Inset: Warburg coefficient as a function of potential.

Having recognized these features, a number of impedance spectra were measured as a function of potential and pH (in the pH range 3–7, i.e. in 0.1 M $KClO_4$ with and without additions of $HClO_4$). The most characteristic impedance behavior can be observed in solutions containing about 0.1 mM $HClO_4$ (around pH 4). These spectra can be well fitted by the equivalent circuit of Fig. 1a (see also Eq. (1)); typical measured spectra, along with the fitted ones—all transformed to complex capacitances—are shown in Fig. 3.

Note that all the spectra are of depressed-arc shape—in both the hydrogen and hydroxide adsorption regions—indicating that the adsorption process is a very fast, i.e. diffusion controlled process. (This is not always so—certain anions adsorb in a slow process [7]). At potentials of the double layer region the arcs shrink into single points, i.e. the adsorption capacitance vanishes and the capacitance is due to double layer charging only. By curve fitting we determined the capacitances and the Warburg parameter; these are compiled and plotted in Fig. 4. Two important conclusions can be drawn:

1. The high frequency (HF) capacitance, identified as C_{dl}, is in the range of 20 μF/cm² everywhere but around 0.1 V versus SCE (≈ 0.6 V vs. RHE) where there is a hump (hereafter denoted as 'capacitance peak').
2. As a check of the diffusion proper, the diffusion coefficient can be calculated from the Warburg coefficient. With $\sigma_{ad} = 400\ \Omega\,cm^2/s^{1/2}$ (cf. the inset of

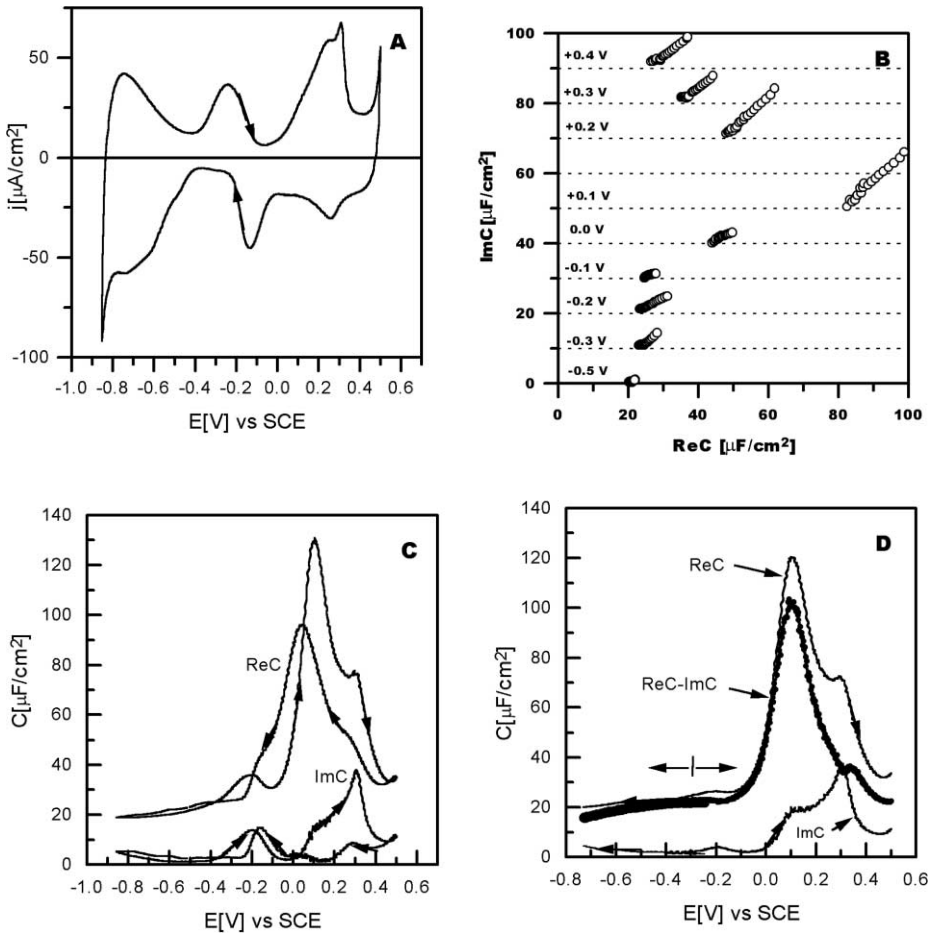

Fig. 5. Pt(111) in 0.1 M $KClO_4$: (a) cyclic voltammogram (100 mV/s, continuous cycling); (b) capacitance spectra (2 Hz–2 kHz) at various potentials (given with respect to SCE); (c) capacitance (1 kHz, 10 mV/s, continuous cycling) as a function of potential; (d) capacitance (1 kHz, 10 mV/s) as a function of potential; scans have started after a 100 s initial delay at -0.3 V. Thick solid line: $C_{dl} \approx \mathrm{Re}\, C - \mathrm{Im}\, C$.

Fig. 4), assuming an electrosorption valency of 1, we obtain a diffusion coefficient of about 6×10^{-5} cm^2/s using Eq. (2)) for both the hydrogen and hydroxide adsorption region. This extraordinarily large diffusion coefficient confirms that H^+ ions are involved in the adsorption process in both regions.

In the following, we concentrate on the double-layer capacitance issues (the diffusion related issues, and the kinetics of adsorption remain to a future publication [7]).

To get accurate $C_{dl}(E)$ curves, we performed a number of impedance measurements in solutions of pH around 4. These revealed that the capacitance-peak location on the SCE scale does not depend on the pH—indicating that this feature is independent of hydrogen or hydroxide adsorption. In order to demonstrate this pH independency, we found additional methods to broaden the experimentally accessible pH range. With these, now we have three options.

Method 1. As explained above, HF capacitances can be determined at low (around 10^{-4} mol/dm^3) H^+ concentrations (i.e. around pH 4) by measuring impedance spectra (Figs. 3 and 4).

Method 2. At very low ($< 10^{-5}$ mol/dm^3) H^+ concentrations—as shown in the paragraph just after Eq. (3)—the spectra shrink into a small region close by C_{dl}. Thus, in neutral or almost neutral perchlorate solutions a single-frequency capacitance measurement using a slow potential scan along with sufficiently high frequency perturbation (say, 10 mV/s, 1 kHz) directly yields the $C_{dl}(E)$ curve. Fig. 5b shows capacitance spectra measured in a neutral solution: the 1 kHz points are very close to the real axis, so the 1 kHz capacitance data (directly, or with minor corrections

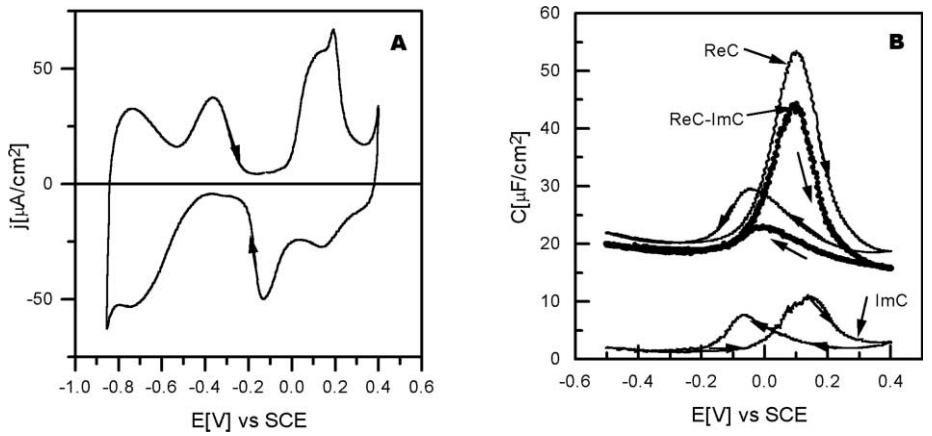

Fig. 6. (a) Cyclic voltammogram (100 mV/s, continuous cycling) of Pt(111) in 0.1 M NaF; (b) Capacitance (1 kHz, 10 mV/s scan rate, continuous cycling) of the same system as a function of potential.

explained later) can be safely regarded as C_{dl}. This method enables one to perform fast measurements—during the time of which the surface remains clean.

Method 3. The peak potential (~ 0.1 V vs. SCE) falls into the double layer region in solutions of pH around 2. Here the adsorption capacitances are zero or close to zero, and thus the overall capacitance (the frequency dependence of which vanishes as the adsorption capacitance approaches zero) is dominated by that of the double layer. Hence in this pH range we can detect the presence of the peak by conventional 18 Hz capacitance measurements.

3.1. Measurements with method 2

The voltammetric behavior of Pt(111) in neutral perchlorate solutions is shown in Fig. 5a. The relatively high currents in the hydrogen and hydroxide adsorption regions still persist; at potentials of the double-layer charging new current peaks appear. By window-opening and stopped-scan experiments one can demonstrate that these peaks and the hysteresis effects are due to local pH changes at the interface [7]. One can eliminate the effect of these local concentration changes (which affect the capacitance curves, too) by halting the potential scan at -0.3 V versus SCE (i.e. just in between the two peaks) and waiting there for about one minute before the subsequent potential scan.

The 1 kHz capacitance measurement yields a capacitance curve, $C_{dl}(E)$, with a certain hysteresis, the origin of which will be discussed elsewhere [7]. There appears a sharp peak at 0.12 V versus SCE (Fig. 5c) during the anodic scan. Note that due to the continuous potential scan, the peak potentials can be determined more precisely than with method 1. Whereas the peak potential during anodic scans is independent of the sweep parameters, the peak location and height during the reverse scan depends on sweep rate and whether or not the sweep has been halted at the positive potential limit (qualitatively, the longer the halt, the larger the hysteresis). To obtain the $C_{dl}(E)$ curve more precisely, we applied two corrections: (i) as in the case of cyclic voltammograms, one can eliminate the hysteresis-related humps by starting the potential scans from -0.3 V with a 100 s initial delay and to record only the forward scans of both directions (Fig. 5d); (ii) the capacitance spectra of this system are approximately of a 45°-line form (Fig. 5b) corresponding to a parallel $C_{dl} - W_{ad}$ circuit. Thus $\mathrm{Re}\, C \approx C_{dl} + 1/(\sigma_{ad}(2i\omega)^{1/2})$; $\mathrm{Im}\, C \approx 1/(\sigma_{ad}(2i\omega)^{1/2})$, hence $C_{dl}(E) = \mathrm{Re}\, C - \mathrm{Im}\, C$. This curve is also plotted in Fig. 5d.

One can get very similar voltammograms and capacitance curves in solutions of NaF (Fig. 6). With this system the capacitance peak is smaller but its location is very close (~ 0.1 V vs. SCE) to that in $KClO_4$ indicating that the peak has—most probably—nothing to do with the chemical nature of the solute.

3.2. Measurements using method 3

A representative curve is shown in Fig. 7. There appears again a hump in the capacitance around 0.1 V versus SCE in the double layer region. One can get such a hump in the pH range 1.5–3 (see also Fig. 8).

We compiled all the representative measurements of the double-layer capacitance relevant to the capacitance peak in Fig. 8. Note that this plot contains capacitance data measured by all three methods, in the pH range 1.5–7.

4. Discussion

There are three messages from this work:

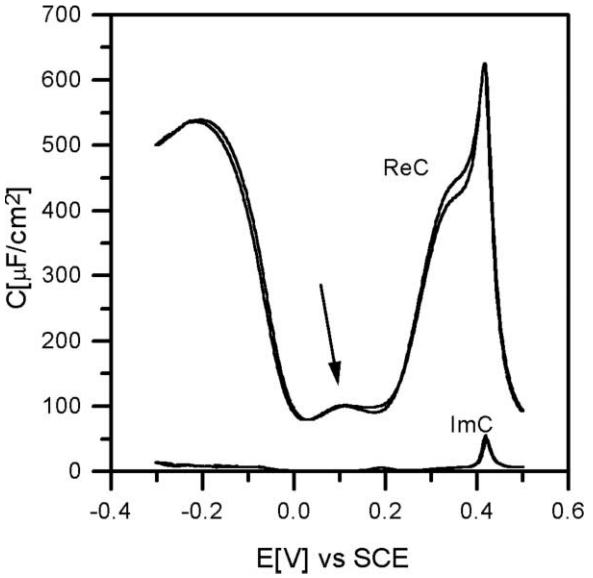

Fig. 7. Capacitance (18 Hz, 10 mV/s scan rate, continuous cycling) as a function of potential of Pt(111) in 0.1 M $KClO_4 + 10$ mM $HClO_4$ (pH ≈ 2). The capacitance hump is shown by the arrow.

1. In general, one cannot directly measure the double-layer capacitance of Pt(111), because the adsorption-related capacitances mask the double-layer capacitance. To avoid this difficulty, one has to measure impedance spectra in solutions containing the adsorbate in low concentrations, and to use the equivalent circuit of Fig. 1a and curve fitting to determine C_{dl}. There are certain cases when special conditions apply allowing the simplification of the measurement (see methods 2 and 3). Apart from these special cases, low concentrations of the adsorbate (< 0.1 mM) are recommended for a precise measurement of C_{dl}.
2. The double-layer capacitance of Pt(111) is of similar value as that of other metals, i.e. it is around the textbook value of 20 μF/cm^2. This is very clearly seen at the cathodic end of the potential range ($E < -0.1$ V vs. SCE). Similar values can be obtained for Pt(111) electrodes covered with adlayers of Cl^-, Br^-, I^- and SO_4^{2-} [7].
3. The $C_{dl}(E)$ plot exhibits a sharp peak at about 0.12 V versus SCE.

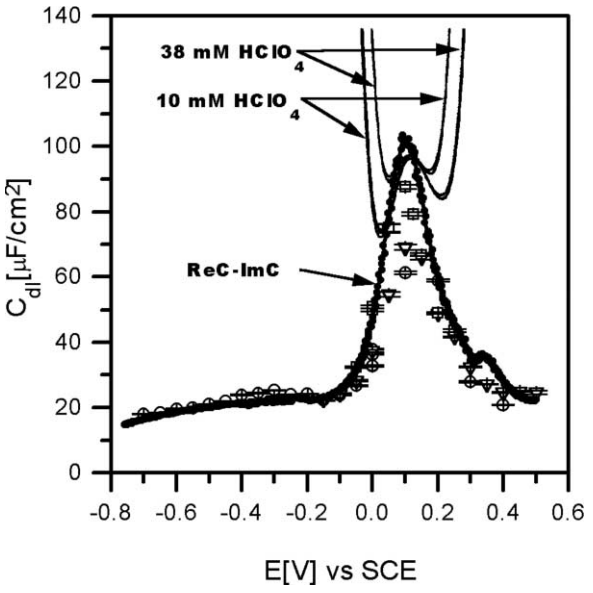

Fig. 8. Double-layer capacitances of Pt(111) in 0.1 M $KClO_4$ (pH 7) as a function of potential obtained from impedance spectra (circles, triangles and squares); and from 1 kHz capacitance measurements (thick solid line). For the sake of completeness, the 18 Hz capacitance data obtained in 0.1 M $KClO_4 + 10$ or 38 mM $HClO_4$ (pH 2 or 1.5, respectively) are also plotted.

In the following, we discuss the possible nature of this peak. First, we stress the fact that the capacitance peak has nothing to do with specific adsorption of H^+ or OH^-, because (i) it has been obtained by separating the double-layer and adsorption-related contributions of the impedance spectra; (ii) at the peak potential there is either no specific adsorption (the peak appears within the double layer region for pH < 3) or in less acidic solutions the hydroxide coverage is still low (< 0.1). Secondly, it is highly improbable that the capacitance peak has something to do with the chemical nature of the solute, since we get similar $C_{dl}(E)$ curves with peaks at the same potential with $KClO_4$ and NaF. Therefore we conclude that the peak is due to some inherent electrical property of the double layer formed by non-specifically adsorbed ions and by the water layer on and close by the platinum surface. We suspect that the peak has some connection with the potential of zero free charge [11] of the Pt(111) electrode.

Such peaks have already been observed on single crystal Au [12] and Ag [13] electrodes. Qualitatively the peak can be interpreted by a dielectric saturation effect: when the potential is sufficiently remote from the pzfc, a significant lowering of the permittivity and therefore of the interfacial capacitance can be expected. We note that these capacitance peaks have been observed only with solutions of high concentrations; at low concentrations we expect a capacitance minimum in accordance with the Gouy–Chapman theory.

Presently, the pzc[1] of the Pt(111) still is a controversial issue. There exists a couple of pzc measurements for the Pt(111)/0.1 M $HClO_4$ system which yield markedly different results. These are as follows:

[1] We use the term pzc (potential zero charge) collectively for pzfc and pztc (potentials of zero free and total charge, respectively).

1. Hamm et al. [14] used an immersion technique. The electrode, cleaned and characterized in an UHV chamber, was immersed in 0.1 M $HClO_4$ under potential control, while the charge flowing through the external circuit was measured. The charge-potential curve, $q(E)$ was shown to be in very good agreement with that derived from voltammetry; it intersected the $q=0$ line at $E=0.84$ V versus RHE. This measurement conformed to the definition of the pztc (point of zero total charge); the pzfc should be even more positive, since at $E=0.84$ V versus RHE the surface is covered by a hydroxide adlayer.
2. Daum et al. [15] stated that the surface is negatively charged up to a potential of 0.86 V versus RHE for Pt(111) in 0.1 M $HClO_4$ by measuring an optical sum frequency generation (SFG) signal.
3. Iwasita et al. [16] reported a sudden change in the IR spectrum at 0.35 V versus RHE in 0.1 M $HClO_4$ solution. They claimed that this is the potential where the water molecules turn upside down, and that this is the pzc. The former statement might be correct, the latter is problematic: the orientation of the water molecules is determined not only by the external electric field, but also by chemical (platinum/water and water/water) interactions.
4. Feliu, Clavilier and coworkers elaborated the CO replacement technique. First they demonstrated that adsorbed I^- ions on Pt(111) can be quantitatively replaced by CO, and by measuring the replacement charge, the amount of adsorbate could be determined with good accuracy [17]. Secondly, it was shown by this technique that various other adsorbates can be replaced, and the CO replacement charge agreed well with the voltammetric charge [18]. Thirdly, Feliu et al. claimed that the potential at which the CO replacement charge is zero, is the pztc. In a tabular form they gave pzc values for various systems, all close to 0.3 V versus RHE; for Pt(111) in 0.1 M $HClO_4$ it was 0.34 V versus RHE [19]. One remark is due here: the CO replacement technique measures the zero point of the adsorbed charges rather than that of the total charge; for determining the pztc a correction for the double layer charge has to be applied. However, this yields only a minor change of the former value (see also Ref. [20]).
5. The present study adds a value of 0.12 V versus SCE to the list. If we assume that the pH independency of the peak in the range of 1.5–7 can be extrapolated also to pH 1 (i.e. the result obtained with acidified 0.1 M $KClO_4$ holds also for 0.1 M $HClO_4$) then we obtain a value for the pzfc of 0.43 V versus RHE for Pt(111) in 0.1 M $HClO_4$.

The above results significantly differ from each other. Further measurements are therefore needed to decide, which values come closest to the real pzc (pztc, pzfc). We suggest (and plan to perform in the near future) two types of measurements:

1. The double layer capacitance for solutions of very low concentrations (say, 1 mM $KClO_4$) should exhibit a sharp minimum at the pzfc in accordance with the Gouy–Chapman theory. We have already carried out capacitance measurements—similar to the one yielding Fig. 5—with lower $KClO_4$ concentrations. These measurements revealed that the capacitance peak decreases with decreasing concentration. However, we could not decrease the concentration to below 10 mM, because the increasing solution resistance masks the capacitive impedance of the interface, thereby increasing the uncertainty of the measurement. For measurements with much lower concentrations a new cell design is needed.
2. The interfacial tension between metal and solution has a maximum at the pztc. To measure interfacial tension, platinum/droplet contact angle measurements are planned.

If the pzfc of Pt(111) were 0.12 V versus SCE, i.e. on the standard hydrogen electrode (SHE) scale $E_{\mathrm{pzfc,SHE}}=0.25+0.12=0.37$ V, then it would have an interesting consequence: we can estimate the potential drop of the surface water dipole layer, χ, by $\chi=(W_{\mathrm{Pt}}-W_{\mathrm{SHE}})/e-E_{\mathrm{pzfc,SHE}}$ where W_{Pt}, and W_{SHE}, are the work functions of Pt(111) and of the SHE, respectively, and e is the elementary charge [21]. W_{Pt} is known to be extremely high (5.8 ± 0.1 eV [22], 5.9 ± 0.1 eV [23]), W_{SHE} is assumed to be 4.5 ± 0.2 eV [24]. Hence, $\chi=[(5.85-4.5-0.37)\pm0.5]=1\pm0.5$ V which seems to be an extraordinarily high value for the water dipole layer potential. (Alternatively, Trasatti's equation $E_{\mathrm{pzfc,SHE}}=W_{\mathrm{PT}}/e-4.61-0.4\alpha$ [21, Eq. (34)] leads to an unusually high value (≈ 2) for the water orientation parameter, α.) We note, however, that molecular dynamics simulations of the Pt(111)/aqueous solution interface predict a 0.7 V contribution of the water molecules to the interfacial potential drop [25,26].

5. Conclusions

1. Double-layer capacitances for Pt(111) can be determined from impedance spectra even in the presence of specific adsorption using the classical adsorption impedance theory. For precise measurements low concentrations of the adsorbate (≤ 0.2 mM) are required.
2. The $C_{\mathrm{dl}}(E)$ plot for Pt(111) in perchlorate solutions exhibits a peak at about 0.12 V versus SCE in the 1.5–7 pH range; from there towards cathodic potentials C_{dl} attains a value of about 20 $\mu F/cm^2$. The peak may be related to the pzfc of Pt(111).
3. The discrepancy between values of the pzc determined by various techniques remains at present.

Acknowledgements

One of us (T.P.) is indebted to the Alexander von Humboldt Foundation for a Research Fellowship and to the Hungarian Research Fund OTKA for financial support under contract T030150. Helpful discussions with Drs Cuesta, Kibler and Schmickler are acknowledged.

References

[1] J. Clavilier, R. Faure, G. Guinet, R. Durand, J. Electroanal. Chem. 107 (1980) 205.
[2] T. Pajkossy, Th. Wandlowski, D.M. Kolb, J. Electroanal. Chem. 414 (1996) 209.
[3] C.C. Herrmann, G.P. Perrault, A.A. Pilla, Anal. Chem. 40 (1968) 1173.
[4] R. Ershler, Disc. Farad. Soc. 1 (1947) 269.
[5] A.N. Frumkin, V.I. Melik-Gaykasyan, Dokl. Akad. Nauk. 5 (1951) 855.
[6] W. Lorenz, Z. Elektrochem. 62 (1958) 192.
[7] T. Pajkossy, D.M. Kolb, to be published.
[8] Z. Kerner, T. Pajkossy, to be published.
[9] J.W. Schultze, F.D. Koppitz, Electrochim. Acta 21 (1976) 327.
[10] K. Al Jaaf-Golze, D.M. Kolb, D. Scherson, J. Electroanal. Chem. 200 (1986) 353.
[11] A.N. Frumkin, O.A. Petrii, B.B. Damaskin, in: J.O'M. Bockris, B.E. Conway, E. Yeager (Eds.), Comprehensive Treatise of Electrochemistry, Plenum Press, New York, 1980, pp. 221–285.
[12] F. Silva, M.J. Sottomayor, A. Hamelin, L. Stoicoviciu, J. Electroanal. Chem. 295 (1990) 301.
[13] G. Valette, J. Electroanal. Chem. 138 (1982) 37.
[14] U.W. Hamm, D. Kramer, R.S. Zhai, D.M. Kolb, J. Electroanal. Chem. 414 (1996) 85.
[15] W. Daum, D. Dederichs, K.A. Friedrich, 50th ISE Meeting, Pavia, Abstract # 855.
[16] T. Iwasita, X. Xia, J. Electroanal. Chem. 411 (1996) 95.
[17] J. Clavilier, R. Albalat, R. Gómez, J.M. Orts, J.M. Feliu, J. Electroanal. Chem. 360 (1993) 325.
[18] J.M. Orts, R. Gómez, J.M. Feliu, A. Aldaz, J. Clavilier, Electrochim. Acta 39 (1994) 1519.
[19] V. Climent, R. Gómez, J.M. Orts, A. Aldaz, J.M. Feliu, in: A. Wieckowski (Ed.), Interfacial Electrochemistry, Marcel Dekker, New York, 1999, p. 463.
[20] M. Weaver, Langmuir 14 (1998) 3932.
[21] S. Trasatti, in: H. Gerischer, C.W. Tobias (Eds.), Advances in Electrochemistry and Electrochemical Engineering, vol. 10, Wiley, New York, 1977, pp. 213–321.
[22] W. Ranke, Surf. Sci. 209 (1987) 57.
[23] M. Kiskinova, G. Pirug, H.P. Bonzel, Surf. Sci. 150 (1985) 319.
[24] S. Trasatti, Pure Appl. Chem. 58 (1986) 955.
[25] G. Nagy, K. Heinzinger, J. Electroanal. Chem. 296 (1990) 549.
[26] G. Nagy, K. Heinzinger, J. Electroanal. Chem. 327 (1992) 25.